ADVANCED FUNCTIONAL MATERIALS
www.afm-journal.de

Flexible Textile Strain Wireless Sensor Functionalized with Hybrid Carbon Nanomaterials Supported ZnO Nanowires with Controlled Aspect Ratio

*Taemin Lee, Wonoh Lee, Sung-Woo Kim, Jae Joon Kim, and Byeong-Su Kim**

Smart fabrics and interactive textiles have attracted great interest as a newly emergent material because of their multifunctional capabilities. Herein, a highly robust wireless flexible strain sensor on the basis of commercial textile by the integration of functional hybrid carbon nanomaterials and piezoresistive material is fabricated. Specifically, a solution-processable spray-assisted coating approach that enables the creation of a uniform coating over a large area of fabrics is employed. The textile-based strain sensor exhibits a highly stable and immediate response over a wide range of bending curvatures and structural properties of ZnO nanowires because of their different deflection behaviors. The wearing performance with attaching on commercial fabrics is further demonstrated. The as-prepared sensor responds well to diverse body motions with accurate detection of strain magnitude and even extends its viability in wireless remote sensing by connecting to a wireless transmitter. The novel approach for the modification of textiles with functional nanomaterials may provide a feasible approach for the production of textile-based electronics without employing any sophisticated fabrication processes, and it further exploits the diverse functionalities by utilizing various sensing components.

1. Introduction

The convergence of electronic components and advanced textiles has led to the emergence of an interdisciplinary field of electronic textiles that brings together the fields like materials science and electronic technologies.[1] Owing to their dimensional advantages such as highly conformal shapes and drapable morphologies, smart fabrics and interactive textiles have attracted immense interest as a newly emergent material in the last few decades in a multitude of applications that include sensing, monitoring, actuating, generating/storing power under external stimuli, and possibly communicating with portable electronic systems through wireless technologies.[2] During the early stages of their development, smart textiles were manufactured by simply attaching commercial thin film electronic components to textile substrates;[3] however, these conventional manufacturing approaches encounter challenges like developing feasible techniques for integrating and transferring the large number of sensing units and processors, and wearing comfort with ease of use. In that regard, smart textiles must be conductive as well as strong, highly deformable, mechanically robust, wearable, and lightweight.

To satisfy the aforementioned conditions, advanced approaches like embedding the electronic functions into pristine fabrics or customizing individual fibers with functional components are highly desired.[4] Tao et al., for example, have demonstrated the integration of desired functionalities into the textile architecture through a direct surface modification of fabrics with functional nanomaterials to produce wearable smart textiles showing multifunctional responses to external stimuli.[5] In other recent example, Cui and co-workers fabricated personal thermal management with metallic nanowire embedded fabrics, which effectively enhancing the insulation performance through the reflection of human body heat radiation due to the presence of metallic nanowire layers.[6] Yun et al. also produced conductive, flexible, and durable textiles wrapped with graphene nanosheets by electrostatic self-assembly, which maintained a high electrical conductivity under severe conditions such as a large number of repetitive bending cycles and even during washing.[7] Thus, the surface modification of commercial textiles with functional nanomaterials can produce smart textiles with potential applications without employing any sophisticated manufacturing processes.

Strain sensors, as one of the representative functions in smart textile, respond to the mechanical deformations caused by the change in electrical characteristics. Such sensors are used

T. Lee, Prof. B.-S. Kim
Department of Energy Engineering
Ulsan National Institute of Science and Technology (UNIST)
50 UNIST-gil, Ulsan 44919, Korea
E-mail: bskim19@unist.ac.kr
Prof. W. Lee
School of Mechanical Engineering
Chonnam National University
77 Yongbong-ro, Buk-gu, Gwangju 61186, Korea
S.-W. Kim, Prof. J. J. Kim
School of Electrical and Computer Engineering
Ulsan National Institute of Science and Technology (UNIST)
50 UNIST-gil, Ulsan 44919, Korea
Prof. B.-S. Kim
Department of Chemistry
Ulsan National Institute of Science and Technology (UNIST)
50 UNIST-gil, Ulsan 44919, Korea

DOI: 10.1002/adfm.201601237

for capturing the posture or motion, measuring biomechanical signals, and detecting respiration. However, conventional metallic strain gauges are not appropriate because of their poor stretchability for large deformations and insufficient sensitivity to conformal geometric changes.[8] Recently, smart sensing textiles have been developed by using carbon-based woven fabrics possessing piezoresistive materials.[9] Carbon-based materials are extensively studied owing to their remarkable mechanical and electrical properties, which satisfy the required characteristics for strain sensing textiles such as highly conductive and mechanically robust.[10] Also, the utilization of piezoresistive materials on textile plays a role as a strain responsive unit due to the lack of a center of symmetry in crystalline structure combined with large electromechanical couplings, which endows a high performance of strain sensing behavior. Originated from the seminal contributions of Wang and co-workers, arrays of ZnO NWs have been widely employed as promising electricity nanogenerators based on the piezoresistive effect.[11] Therefore, highly flexible and sensitive strain sensors utilizing carbon nanomaterials along with piezoresistive sensing materials are expected to play a key role in personal health monitoring, human-benign devices, and highly sensitive robot sensors.

Herein, we fabricated a highly robust wireless flexible strain sensor based on commercial textiles by assembling functional hybrid carbon nanomaterials and piezoresistive ZnO NWs on a textile substrate (**Figure 1**). Specifically, a solution-processable spray-assisted coating approach was employed to create a uniform coating of ZnO NWs over a large surface area of fabrics. The assembly of hybrid carbon nanomaterials provides highly conducting channels with excellent stability toward mechanical bending and deforming. A facile one-step hydrothermal method utilizing the self-organized growth of ZnO NWs irrespective of the substrate was employed to grow ZnO NWs on the top of reduced graphene oxide (rGO) layers.[12] More interestingly, the piezoresistive functions of the individual ZnO NWs are critically linked to their geometrical features due to the difference in their deflection behaviors.[13] In this study, we systematically explored piezoresistive strain sensing performance depending on the morphological transition from seed particle to nanowires by varying the aspect ratio (AR) of ZnO structure. The resulting sensor clearly demonstrated a good strain responsive behavior with a linear current change as a function of bending curvature and structural properties of the ZnO NWs, which has not been explored in this field, particularly on the textile platform.

Thus, our novel approach for modification of textiles with functional nanomaterials may provide a highly attractive tool for the production of textile-based electronics without employing any sophisticated fabrication processes. Furthermore, smart textiles offer a suitable platform for human interface as they conform to the shape of the human body. It allows a facile access to the diverse functionalities on the electronic components by utilizing the various sensing components and it even enables remote monitoring with the wireless communication technology.

2. Results and Discussion

A textile-based strain sensor modified with hybrid nanomaterials was initially assembled by the spray-assisted coating process onto a commercial textile (Figure 1). To produce a mechanically bendable and flexible conducting substrate, we modified the surface of the PET (polyethylene terephthalate) textile with hybrid carbon nanomaterials based on multiwalled carbon nanotubes (CNT) and reduced graphene oxide (rGO) nanosheets. Prior to the assembly of hybrid carbon nanomaterials, the pristine PET textile was treated with oxygen plasma to endow hydrophilic surface that allows strong binding with functional materials without delamination.[14] Chemically modified CNT suspension was subsequently coated on the surface of the PET textile, which resulted in the formation of continuous conducting networks with high mechanical durability. The rGO layers were then assembled to produce interconnected conducting networks utilizing the synergistic dimensional commensurate effect between 1D and 2D nanomaterials.

The integration of electronic functionalities into textiles is vital for the future of wearable electronics, while retaining the desirable characteristics such as flexibility, strength, and conductivity. Because of their exceptional structural, mechanical, and electrical properties, these hybrid carbon nanomaterials are considered one of the most promising flexible electrode materials to alternating the commercial ITO-coated electrodes that possesses limited flexibility and inherent fragility. We examined the mechanical durability of the prepared electrodes by measuring the resistance changes with respect to the repeated bending–release cycles (Figure S1, Supporting Information). In contrast to an ITO-coated PET electrode, the hybrid CNT/rGO electrode fabricated in this study exhibited an excellent structural flexibility with negligible changes (3–5%) in sheet resistance after over 100 bending–release cycles.

Furthermore, the modification of textile substrates using 2D graphene sheets provides an excellent platform for the growth of other functional nanomaterials. Hence, well-aligned ZnO NWs could be successfully grown on the modified textile substrate. We found that the quality of the NW growth was severely affected by the use of rGO as a top substrate on the textile substrate (Figure S2, Supporting Information). Finally, a polydimethylsiloxane (PDMS) polymeric layer was embedded into the aligned ZnO structure to prevent the deformation of the sensor assembly from the external mechanical stress (Figure S3, Supporting Information).

The scanning electron microscopy (SEM) images of the modified PET textile samples showed that the entire surface was evenly coated with the functional nanomaterials without the formation of any noticeable aggregates (**Figure 2**). Typically, the pristine PET textile shows evenly arranged fibers with a diameter of 40 μm and large regular rectangular pores (50 × 50 μm^2). After modification with the hybrid CNT/rGO carbon nanomaterials, the surface morphology of the fiber exhibited a wrinkled structure, indicating a successful deposition of the rGO nanosheets onto the pristine PET textiles. After the growth of ZnO NWs, highly uniform and densely packed array of ZnO NWs on the top of the graphene surface was confirmed by SEM.

The piezoresistive properties of the ZnO strongly depend on their microstructure which includes the crystal size, orientation and morphology, aspect ratio, and even crystalline density. The growth rate of a face is controlled by the combination

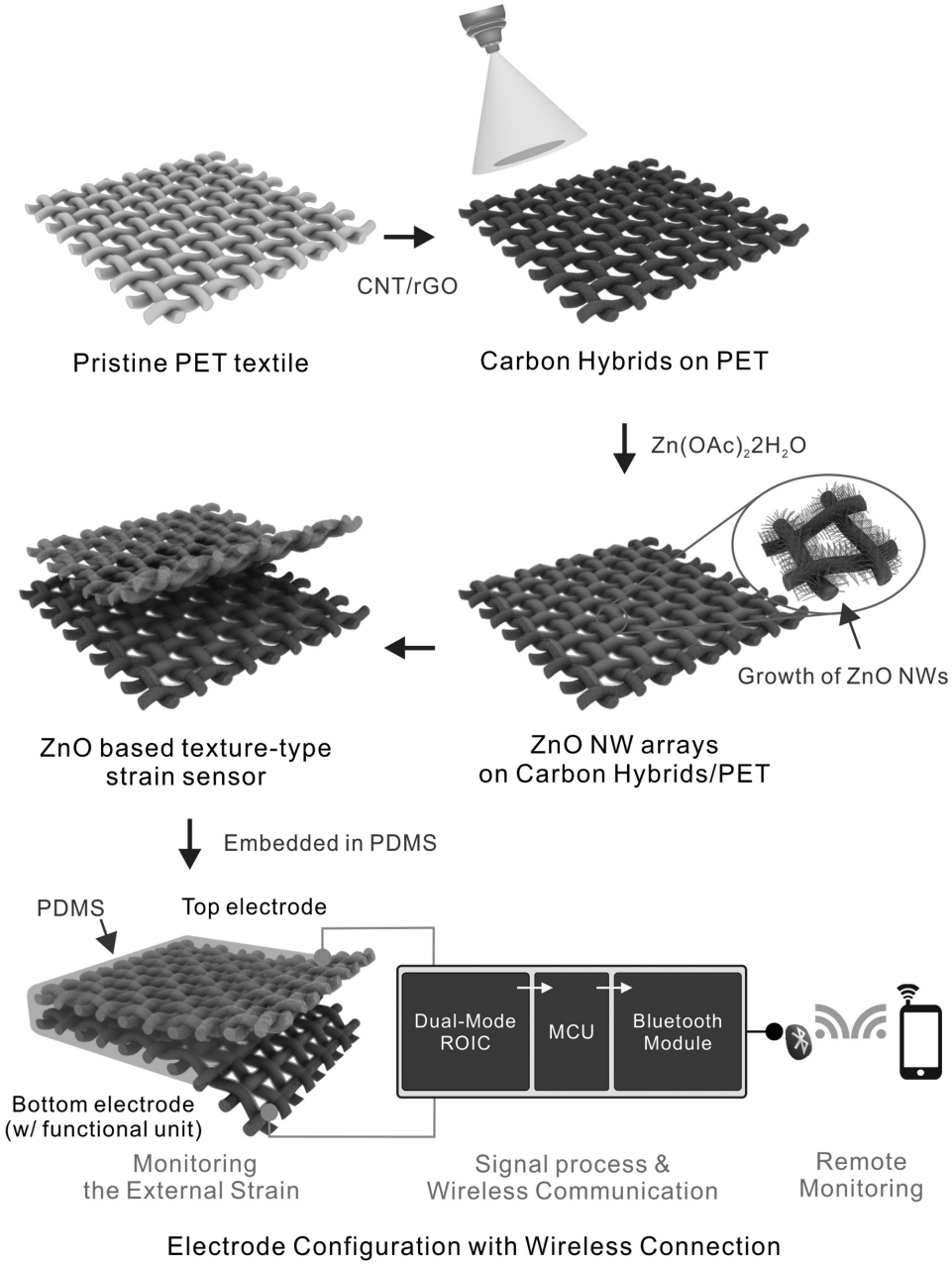

Figure 1. Schematic illustration of the modification of pristine PET textile with functional nanomaterials for flexible textile-based strain sensor with wireless monitoring system.

of the internal, structurally related (intermolecular binding preferences), and external factors (supersaturations, temperature, solvents, and additives).[15] Hence, we investigated the effect of the morphological transitions of the ZnO structure, which depends on the AR, from seed particles to rods and eventually to nanowires, on the piezoresistive strain sensing performance of the sensor obtained in this study. The structure of the ZnO NWs was highly tunable and depended on the reaction time (*h*) in the growth bath of ZnO NWs. The resulting ZnO NW was denoted as ZnO-*h* depending on the reaction time, for example, ZnO-0 (seed only) and ZnO-3 (for a growth time of 3 h).

The cross-sectional SEM images of the NW arrays suggested that the ZnO NWs grew nearly vertically on the seed layer coated on a silicon substrate (**Figure 3**a). The average size of the ZnO NWs increased with the reaction time, for example, when the reaction time increased from 0 to 5 h, the ZnO NWs grew up to 40–80 nm in diameter and 0.3–2 µm in length (Figure 3b). The AR of the ZnO NWs defined as the length-to-diameter ratio also underwent a gradual increase with the reaction time. The highest AR obtained in this study was ≈25 (Figure 3c). At the onset of the growth period, vertical growth (polar surface) along the *c*-axis of the ZnO crystalline structure appears to be more significant than the lateral growth (non-polar surface).

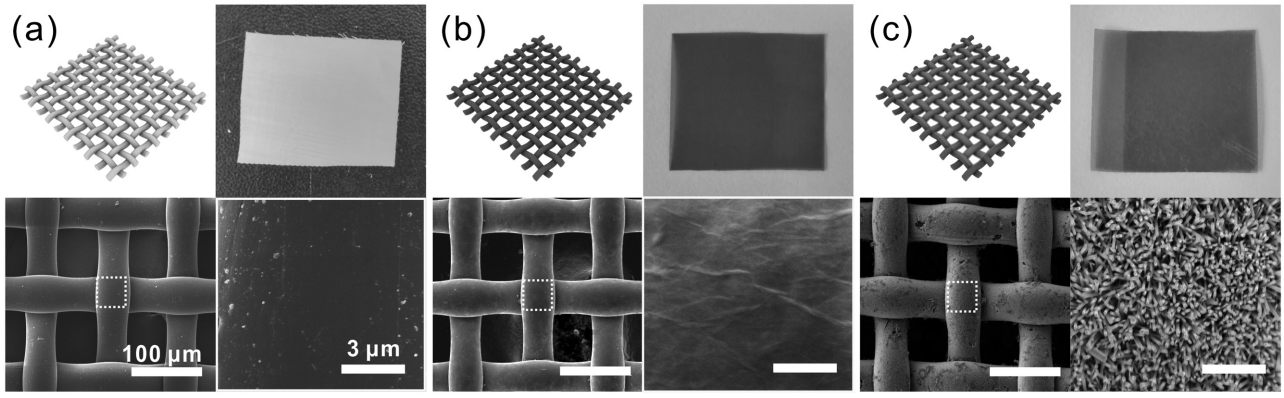

Figure 2. a–c) (Top) Digital photographs of the prepared textile-based strain sensors and (bottom) low and high magnification of the SEM images representing the surface morphology of each sample. a) PET textile, b) hybrid CNT/rGO coated PET textile, and c) ZnO NWs grown onto the surface of the individual PET textile fiber with high uniformity.

When the growth time exceeded 5 h, the length of the ZnO NWs became almost independent of the growth time, while the diameter slightly increased. This could be attributed to the relative growth rates of the polar and nonpolar surfaces, which can be readily tuned by varying the growth time.[16]

In order to verify the strain response properties of the textile-based strain sensor with different geometries of ZnO nanostructures, we investigated the electromechanical performance by mounting the as-prepared strain sensor on a bending machine (**Figure 4**a and Figure S4, Supporting Information). Specifically, the static state electromechanical properties of the strain sensor were measured by monitoring the current changes ($\Delta I/I_0$) under different strain states at a fixed potential of 5 V. We checked the current flow through the device by changing the bending radius (R) of the device step by step from R_0 (flat state) to R_6 (highly curved state of with R = 6.9 mm) (Figure S5 and Table S1, Supporting Information). The textile-based strain sensor was embedded in the elastomeric PDMS

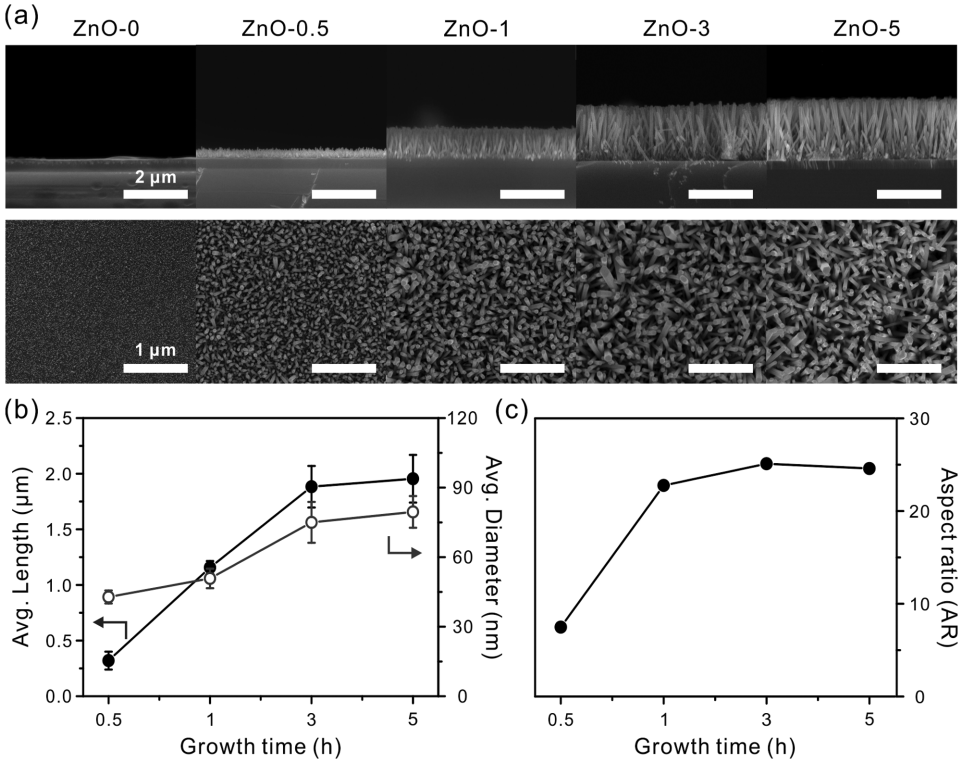

Figure 3. a) Representative SEM images of the ZnO NW arrays prepared with varying reaction times (h). Note that the ZnO-h represents the NWs obtained after the different growth time. b) Average length and diameter of the ZnO NWs with respect to the growth time (averaged over 100 samples). c) Aspect ratio of the ZnO NWs with respect to the growth time.

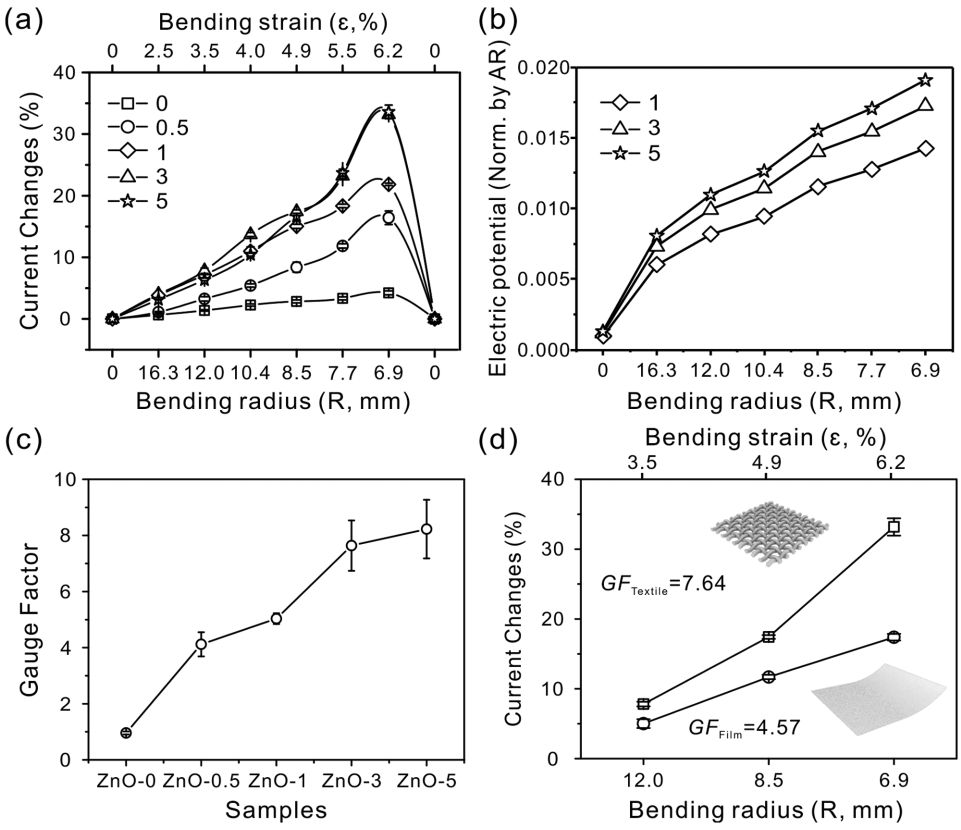

Figure 4. a) Strain-responsive current changes of various ZnO-*h* nanostructures under varying bending conditions. b) Electrical potential normalized by AR of ZnO nanostructure with respect to a bending radius calculated by a simple analytical approach. The numbers in (a) and (b) indicate the reaction time (*h*) of ZnO nanostructure. c) Calculated gauge factor of each ZnO-*h* nanostructure obtained by averaging ten repeated individual measurements. d) Comparison of strain-responsive sensing performance of ZnO-3 assembled on the PET textile and the PET film. The gauge factor (GF) of the ZnO NWs assembled on the textile substrate is about twice as high as that of those assembled on a plain ZnO film.

layer to prevent the structural deformation. Since the elastomeric patch can be easily bent and deformed, it could deliver the bending–release motions to the strain sensor. All the prepared samples exhibited a good strain responsive behavior in which current change was linearly proportional to the function of the bending radius and a good recovery performance without degradation after retracing to the initial state. It is interesting to note the strain responsive performance with respect to the AR of the ZnO nanostructures. For example, the value of the current change increased considerably from ≈15% (ZnO-0.5) to ≈33% (ZnO-3 and ZnO-5) at a high curvature of R_6 state. On the contrary, ZnO-0 with only ZnO seed particles deposited on the hybrid CNT/rGO carbon electrode exhibited a negligible change of ≈3% under the identical bending states, indicating a strong contribution of AR of the ZnO NWs to the electromechanical sensitivity.

This finding can be interpreted by the geometrical features of the ZnO nanostructure. The elastic modulus of the individual NWs could be affected from the size and length of the NWs because of the different deflection behavior of the cantilever.[11a,17] Similarly, the mechanical properties of the individual NWs of different lengths were investigated in an aligned array. Thus, we postulate that the NW structure with a high AR is relatively more curved, bendable, and stretchable than those with a lower AR, resulting that generates higher polarized charge potentials, which is strongly attributed to the variable strain sensing capability with the relative current changes correlated with the quantity of the applied mechanical stress.

Such a dependence of the current change on the AR of the ZnO NWs can also be deduced by considering a simple analytical approach. Under a bending mode of the device, a bending strain of the ZnO NW can be regarded as a unit value of deflection at the NW tip. According to the elemental elasticity theory,[18] the lateral force f_{tip} at the NW tip is related to the maximum deflection (δ_{max}) according to Equation (1)

$$\delta_{max} = \frac{f_{tip} l^3}{3EI} \tag{1}$$

where E, I, and l are the elastic modulus, the moment of inertia, and the length of the ZnO NW, respectively. By considering that the ZnO NW has a cylindrical shape with a diameter of d, the lateral force is expressed as given in Equation (2)

$$f_{tip} \approx \frac{d^4}{Rl^2} \frac{N_Z}{w\rho_Z} \tag{2}$$

where N_Z and ρ_z are the number and areal density of the NWs in the bent device, and w is the width of the device. Wang and Gao showed that the maximum electrical potential δ_{max} has a

linear relationship with f_{tip}/d.[19] Therefore, the potential of the ZnO NW by bending the device is reduced as expressed in Equation (3)

$$\varphi_{max} \approx \frac{l}{R(l/d)^3}\frac{N_Z}{w\rho_Z} \quad (3)$$

In Figure 4b, the normalized electrical potentials for ZnO-1, ZnO-3, and ZnO-5 are plotted using Equation (3) with an assumption that the number and density of the NWs are identical for all the cases. Note that ZnO-0 and ZnO-0.5 were excluded from this calculation as these samples have too small and short nanostructures which may lead to imperfect contact to electrodes, which in turn leads to a reduction in the number (N_Z) of active NWs. Similar to Figure 4a, the electrical potential increases with respect to the bending strain (or curvature). Even though the three different ZnO nanostructures have similar ARs, the longer ZnO NWs show a higher potential in general.

Based on the electromechanical performance, the gauge factor (GF) of the textile-based strain sensor can be calculated using Equation (4)

$$GF = \frac{\Delta R/R}{\varepsilon} = \frac{\Delta i/i_f}{\varepsilon} = \frac{(i_0 - i_f)}{i_f \times \varepsilon} \quad (4)$$

where ε, i_0, and i_f denote the strain applied to the sensor, initial current at zero strain, and final current at ε strain, respectively. Similar to the trend observed for the current changes, the GF values also depended on the growth time of the ZnO nanostructures (Figure 4c). For example, the GF value is ≈0.96 for ZnO-0 and ≈7.64 for ZnO-3. These values are comparable to those for the commercial strain gauges including metal-foil (2–5), thin-film metal (≈2),[20] polysilicon (≈30),[21] and thick-film resistors (≈100).[22]

Comparison of the performance of the PET textile substrate with that of conventional PET based film was accomplished by assembling ZnO-3 NW on the PET textile substrate as well as the conventional PET film (Figure 4d). Interestingly, the GF of the PET textile (≈7.64) was found to be two times higher than that of the PET film (≈4.57), which strongly advocates the use of unique fabric-like architectures with high flexibility and deformability under extreme bending states as suitable substrates for developing strain sensors.

To evaluate the mechanical durability of the textile-based strain sensor, we monitored their response and recovery properties at a constant strain state with the varying bending rates of 0.2, 0.4, and 1 Hz (**Figure 5**). Our device maintained a superior response and recovery properties even under high strain which indicates an attractive perspective in the applications such as precision measurement over multiple cycles of usage. The frequency of response corresponds well with the frequency of excitation; a consistent behavior in the response of the sensor is observed for different frequencies tested. Therefore, the modified textile-based strain sensor possesses highly stable architectures without any structural degradation, which can be potentially applicable to other sensing devices with proper sensing units.

Wearable electronics that monitor the external physical/chemical stimuli, and actuating or possibly communicating to other electronic devices are the next frontiers in the personal health monitoring and human-benign devices. To demonstrate the potential of the textile-based strain sensor in wearable devices, the as-fabricated strain sensor was attached onto the fabrics and its electromechanical sensing performance with diverse motions in different parts of the human body was monitored (**Figure 6**a and Figure S6, Supporting Information). A highly flexible and durable textile-based strain sensor can be easily implanted in the commercial fabrics, which then responds to the bending–release motion of the elbow and fingers, and also the output current signal well recovered to the original value. It can also be seen that the current switched rapidly at every turning point; the current maintained identical under the same motion and no remarkable current change was observed at a certain strain state. We can thus achieve an accurate detection using the as-prepared textile-based strain sensor owing to its high flexibility and linear piezoresistivity behavior.

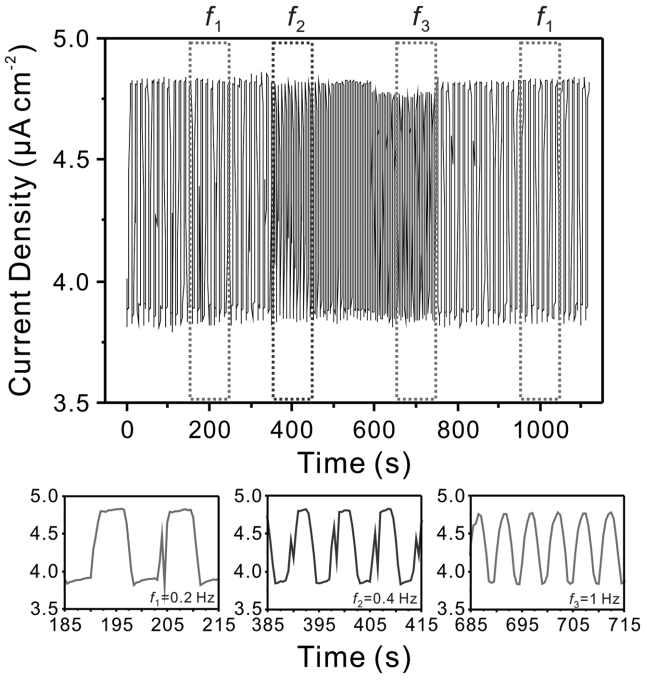

Figure 5. Electromechanical durability of the textile-based strain sensor at different rates of bending–release frequency varying from 0.2 to 1 Hz. The ZnO-3 based strain sensor was tested at a constant bending state (R_4) for overall 200 cycles. Each frequency was tested for 50 cycles.

Furthermore, the wireless interface for the textile strain sensor was implemented by utilizing a readout integrated circuit (ROIC), a microcontroller unit (MCU), and a Bluetooth module (Figure S7, Supporting Information). Instant variations in the strain sensor are detected by the ROIC and converted to corresponding digital data by the MCU such that they are wirelessly transmitted to a mobile phone through the Bluetooth connectivity and displayed through mobile application software. The ROIC was designed to have a dual-mode structure that is composed of a programmable potentiometer, a programmable current source, and a controller (Figure S8, Supporting Information).[23] In this way, the bending-induced strain output signals were wirelessly transmitted to mobile phones through the wireless sensor interface module. It clearly exhibited the

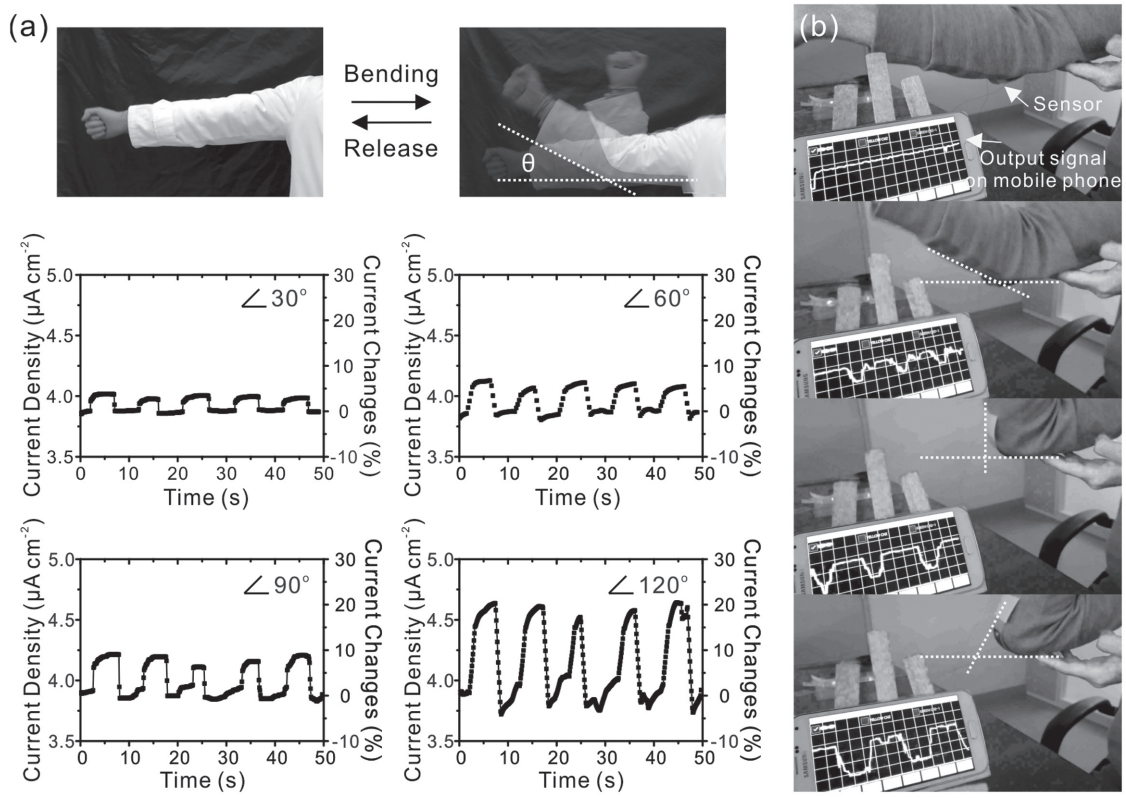

Figure 6. a) Strain-responsive sensing performance of the ZnO-3 strain sensor that was attached on an elbow under different bending angles. b) Remote monitoring and wireless communication with mobile phone via connecting the Bluetooth modules.

on/off strain sensing behavior under the bending–release period (Movie S1, Supporting Information). In addition, when the textile-based strain sensor was bent at different angles (45°, 90°, and 120°), it produced output signals with different intensities since the larger bending motions resulted in greater elongations of the sensor (Figure 6b and Movie S2, Supporting Information). The proportional increase in the relative current change with the bending angle means that the sensor has the capability to detect as well as quantify the applied bending strain. As a consequence, the textile-based strain sensor performed well even while being worn on the body, which is beneficial for personal health monitoring and human-benign devices.

Current advances in wearable technologies, new materials, nanotechnology, and miniaturized electronics are making wearable systems more feasible. However, the comfort during wearing is the key factor for the widespread acceptance of such devices. Textiles represent an indispensable component in our daily life and provide an attractive platform for future wearable electronics because of their myriad shapes with flexible and stretchable characteristics. Besides, devices with multifunctional capabilities can be developed by facile integration of the desired functionalities into the textile architecture. Therefore, we anticipate that the rational design of hybrid integrations into the textile platform opens up the possibility for the production of diverse textile-based devices with wearing comfort and ease of use.

3. Conclusion

In summary, we developed a highly robust textile-based wireless flexible strain sensor on by integrating functional hybrid carbon nanomaterials and ZnO NWs with piezoresistive effect into the textile substrate. We systematically investigated the dependence of bending-induced strain sensing behavior on the morphological transition of ZnO structure depending on the AR from seed particle to nanowires because the piezoresistive properties of the individual ZnO NWs are depended on their geometrical features. The textile-based strain sensor exhibited a highly stable and immediate response over a wide range of bending curvatures and structural properties of the ZnO NWs, resulting that are well consistent with the geometrical effect of ZnO NWs due to the different deflection behavior. Furthermore, we demonstrated the general performance of the as-prepared sensor while attached it to the commercial fabrics. A rapid response to the diverse motions of the human body with accurate detections of the quantity of the applied bending strain was observed. Finally, the performance of the sensor was extended when connected to a wireless transmitter, which demonstrated the viability in wireless communication and remote monitoring even while being worn on the body. Therefore, our novel approach for the modification of textiles with functional nanomaterials may provide a highly attractive approach for the production of textile-based electronics without employing any sophisticated fabrication processes, and further enables the

extended and diverse functionalities by utilizing with various sensing components.

4. Experimental Section

Fabrication of CNT/rGO Wrapped PET Textiles: The preparation of chemically modified CNT and rGO suspensions is described in previous reports.[24] A PET textile (TEXTOMA Co., South Korea) was thoroughly cleaned before use by successive sonication in acetone, isopropanol, and deionized water for 10 min and then treated with oxygen plasma to introduce a hydrophilic surface. First, the CNT wrapped PET textile was prepared by spray-assisted coating with chemically modified CNT suspension, which resulted in conducting channels with high flexibility. Subsequently, chemically exfoliated rGO suspension was coated on the surface of PET/CNT textile thus providing a continuous conducting network and a platform for the growth of ZnO NW arrays. Finally, the hybrid CNT/rGO substrate was dried at 60 °C overnight to increase the mechanical integrity of the entire film.

Growth of ZnO NW Arrays on CNT/rGO Wrapped PET Textiles: The ZnO nanocrystals were prepared according to the method developed by Pacholski et al.[25] A KOH solution in methanol (30×10^{-3} M) was added slowly to a solution of zinc acetate dihydrate (10×10^{-3} M) in methanol at 60 °C and stirred for 2 h. Well-aligned ZnO nanowire arrays were grown using a simple two-step process. In the first step, ZnO nanocrystals (5–10 nm in diameter) were spray-coated onto the surface of CNT/rGO coated PET textiles to form a crystal seed. Once the coating was done, the hydrothermal ZnO growth was carried out by dipping the coated substrate in an aqueous solution of zinc nitrate hydrate (25×10^{-3} M) and hexamethylenetetramine (25×10^{-3} M) at 90 °C. An array of ZnO NWs was prepared with various ARs by varying the reaction time from 0.5 to 5 h.

Strain Sensor Measurements: Teflon-coated copper wires were connected to each end of the as-prepared textile strain sensor and PDMS was used to pack the device. The typical current–time (*I*–*t*) measurements of the device under different strains were carried out on a potentiostat (VSP, Bio-Logic., USA) with a constant applied potential of 5 V. The device was placed and fixed on two separate mechanical bending machines and the change in electrical resistance with different bending radii and during the repeated bending–release cycles was examined.

Supporting Information

Supporting Information is available from the Wiley Online Library or from the author.

Acknowledgements

This work was supported by the National Research Foundation of Korea (NRF) Grants (NRF-2014R1A2A1A11052829 and 2015R1A2A2A04003160).

Received: March 10, 2016
Revised: May 29, 2016
Published online: July 1, 2016

[1] a) D.-H. Kim, J. A. Rogers, *Adv. Mater.* **2008**, *20*, 4887; b) D. Marculescu, R. Marculescu, N. H. Zamora, P. Stanley-Marbell, P. K. Khosla, S. Park, S. Jayaraman, S. Jung, C. Lauterbach, W. Weber, T. Kirstein, D. Cottet, J. Grzyb, G. Troster, M. Jones, T. Martin, Z. Nakad, *Proc. IEEE* **2003**, *91*, 1995; c) W. Zeng, L. Shu, Q. Li, S. Chen, F. Wang, X.-M. Tao, *Adv. Mater.* **2014**, *26*, 5310.

[2] a) M. K. Choi, I. Park, D. C. Kim, E. Joh, O. K. Park, J. Kim, M. Kim, C. Choi, J. Yang, K. W. Cho, J.-H. Hwang, J.-M. Nam, T. Hyeon, J. H. Kim, D.-H. Kim, *Adv. Funct. Mater.* **2015**, *25*, 7109; b) J. Lee, H. Kwon, J. Seo, S. Shin, J. H. Koo, C. Pang, S. Son, J. H. Kim, Y. H. Jang, D. E. Kim, T. Lee, *Adv. Mater.* **2015**, *27*, 2433; c) J. J. Park, W. J. Hyun, S. C. Mun, Y. T. Park, O. O. Park, *ACS Appl. Mater. Interfaces* **2015**, *7*, 6317; d) W. Seung, M. K. Gupta, K. Y. Lee, K.-S. Shin, J.-H. Lee, T. Y. Kim, S. Kim, J. Lin, J. H. Kim, S.-W. Kim, *ACS Nano* **2015**, *9*, 3501; e) L. Hu, M. Pasta, F. L. Mantia, L. Cui, S. Jeong, H. D. Deshazer, J. W. Choi, S. M. Han, Y. Cui, *Nano Lett.* **2010**, *10*, 708.

[3] a) G. Schwartz, B. C. K. Tee, J. Mei, A. L. Appleton, D. H. Kim, H. Wang, Z. Bao, *Nat. Commun.* **2013**, *4*, 1859; b) A. N. Sokolov, B. C. K. Tee, C. J. Bettinger, J. B. H. Tok, Z. Bao, *Acc. Chem. Res.* **2012**, *45*, 361; c) H. S. Lee, J. Chung, G.-T. Hwang, C. K. Jeong, Y. Jung, J.-H. Kwak, H. Kang, M. Byun, W. D. Kim, S. Hur, S.-H. Oh, K. J. Lee, *Adv. Funct. Mater.* **2014**, *24*, 6914; d) G.-T. Hwang, J. Yang, S. H. Yang, H.-Y. Lee, M. Lee, D. Y. Park, J. H. Han, S. J. Lee, C. K. Jeong, J. Kim, K.-I. Park, K. J. Lee, *Adv. Energy Mater.* **2015**, *5*, 1500051.

[4] M. Stoppa, A. Chiolerio, *Sensors* **2014**, *14*, 11957.

[5] a) J.-W. Jeong, W.-H. Yeo, A. Akhtar, J. J. S. Norton, Y.-J. Kwack, S. Li, S.-Y. Jung, Y. Su, W. Lee, J. Xia, H. Cheng, Y. Huang, W.-S. Choi, T. Bretl, J. A. Rogers, *Adv. Mater.* **2013**, *25*, 6839; b) W.-H. Yeo, Y.-S. Kim, J. Lee, A. Ameen, L. Shi, M. Li, S. Wang, R. Ma, S. H. Jin, Z. Kang, Y. Huang, J. A. Rogers, *Adv. Mater.* **2013**, *25*, 2773; c) M. El-Sherif, X. Tao, *Wearable Electronics and Photonics*, Woodhead Publishing, Cambridge **2005**; d) X. Tao, *Smart Fibres, Fabrics and Clothing: Fundamentals and Applications*, Woodhead Publishing, Cambridge **2001**; e) X. Tao, L. Tang, W.-C. Du, C.-L. Choy, *Compos. Sci. Technol.* **2000**, *60*, 657.

[6] P.-C. Hsu, X. Liu, C. Liu, X. Xie, H. R. Lee, A. J. Welch, T. Zhao, Y. Cui, *Nano Lett.* **2015**, *15*, 365.

[7] Y. J. Yun, W. G. Hong, W.-J. Kim, Y. Jun, B. H. Kim, *Adv. Mater.* **2013**, *25*, 5701.

[8] a) D. J. Cohen, D. Mitra, K. Peterson, M. M. Maharbiz, *Nano Lett.* **2012**, *12*, 1821; b) M. Hempel, D. Nezich, J. Kong, M. Hofmann, *Nano Lett.* **2012**, *12*, 5714; c) T. Yamada, Y. Hayamizu, Y. Yamamoto, Y. Yomogida, A. Izadi-Najafabadi, D. N. Futaba, K. Hata, *Nat. Nanotechnol.* **2011**, *6*, 296.

[9] a) C. K. Jeong, J. Lee, S. Han, J. Ryu, G.-T. Hwang, D. Y. Park, J. H. Park, S. S. Lee, M. Byun, S. H. Ko, K. J. Lee, *Adv. Mater.* **2015**, *27*, 2866; b) J.-H. Lee, K. Y. Lee, M. K. Gupta, T. Y. Kim, D.-Y. Lee, J. Oh, C. Ryu, W. J. Yoo, C.-Y. Kang, S.-J. Yoon, J.-B. Yoo, S.-W. Kim, *Adv. Mater.* **2014**, *26*, 765; c) J.-H. Lee, K. Y. Lee, B. Kumar, N. T. Tien, N.-E. Lee, S.-W. Kim, *Energy Environ. Sci.* **2013**, *6*, 169; d) K.-I. Park, M. Lee, Y. Liu, S. Moon, G.-T. Hwang, G. Zhu, J. E. Kim, S. O. Kim, D. K. Kim, Z. L. Wang, K. J. Lee, *Adv. Mater.* **2012**, *24*, 2999.

[10] a) A. K. Geim, K. S. Novoselov, *Nat. Mater.* **2007**, *6*, 183; b) K. S. Novoselov, A. K. Geim, S. V. Morozov, D. Jiang, Y. Zhang, S. V. Dubonos, I. V. Grigorieva, A. A. Firsov, *Science* **2004**, *306*, 666; c) S. Stankovich, D. A. Dikin, G. H. B. Dommett, K. M. Kohlhaas, E. J. Zimney, E. A. Stach, R. D. Piner, S. T. Nguyen, R. S. Ruoff, *Nature* **2006**, *442*, 282.

[11] a) Z. L. Wang, J. Song, *Science* **2006**, *312*, 242; b) X. Xiao, L. Yuan, J. Zhong, T. Ding, Y. Liu, Z. Cai, Y. Rong, H. Han, J. Zhou, Z. L. Wang, *Adv. Mater.* **2011**, *23*, 5440.

[12] a) N. H. Alvi, M. Riaz, G. Tzamalis, O. Nur, M. Willander, *Solid-State Electron.* **2010**, *54*, 536; b) A. Khan, M. Ali Abbasi, M. Hussain, Z. Hussain Ibupoto, J. Wissting, O. Nur, M. Willander, *Appl. Phys. Lett.* **2012**, *101*, 193506; c) A. Khan, M. Hussain, M. A. Abbasi, Z. H. Ibupoto, O. Nur, M. Willander, *J. Mater. Sci.* **2014**, *49*, 3434; d) M. Willander, O. Nur, Q. X. Zhao, L. L. Yang, M. Lorenz, B. Q. Cao, J. Z. Pérez, C. Czekalla, G. Zimmermann, M. Grundmann, A. Bakin, A. Behrends, M. Al-Suleiman, A. El-Shaer,

A. C. Mofor, B. Postels, A. Waag, N. Boukos, A. Travlos, H. S. Kwack, J. Guinard, D. L. S. Dang, *Nanotechnology* **2009**, *20*, 332001.
[13] a) A. B. Djurišić, Y. H. Leung, *Small* **2006**, *2*, 944; b) K. Liu, W. Wu, B. Chen, X. Chen, N. Zhang, *Nanoscale* **2013**, *5*, 5986; c) C. Xu, P. Shin, L. Cao, D. Gao, *J. Phys. Chem. C* **2010**, *114*, 125; d) J. Zhang, H. Liu, Z. Wang, N. Ming, Z. Li, A. S. Biris, *Adv. Funct. Mater.* **2007**, *17*, 3897; e) Q. Zhao, H. Z. Zhang, Y. W. Zhu, S. Q. Feng, X. C. Sun, J. Xu, D. P. Yu, *Appl. Phys. Lett.* **2005**, *86*, 203115.
[14] a) T.-K. Hong, D. W. Lee, H. J. Choi, H. S. Shin, B.-S. Kim, *ACS Nano* **2010**, *4*, 3861; b) K. Jo, T. Lee, H. J. Choi, J. H. Park, D. J. Lee, D. W. Lee, B.-S. Kim, *Langmuir* **2011**, *27*, 2014.
[15] a) H. L. Cao, X. F. Qian, Q. Gong, W. M. Du, X. D. Ma, Z. K. Zhu, *Nanotechnology* **2006**, *17*, 3632; b) B. Cheng, E. T. Samulski, *Chem. Commun.* **2004**, 986; c) J. Joo, B. Y. Chow, M. Prakash, E. S. Boyden, J. M. Jacobson, *Nat. Mater.* **2011**, *10*, 596; d) U. Galan, Y. Lin, G. J. Ehlert, H. A. Sodano, *Compos. Sci. Technol.* **2011**, *71*, 946.
[16] a) S. Xu, C. Lao, B. Weintraub, Z. L. Wang, *J. Mater. Res.* **2008**, *23*, 2072; b) S. Xu, Z. L. Wang, *Nano Res.* **2011**, *4*, 1013; c) Z. R. Tian, J. A. Voigt, J. Liu, B. McKenzie, M. J. McDermott, M. A. Rodriguez, H. Konishi, H. Xu, *Nat. Mater.* **2003**, *2*, 821.
[17] J. Song, X. Wang, E. Riedo, Z. L. Wang, *Nano Lett.* **2005**, *5*, 1954.
[18] S. Timoshenko, J. Goodier, *Theory of Elasticity*, 3rd ed., McGraw-Hill, New York **1970**.
[19] Y. Gao, Z. L. Wang, *Nano Lett.* **2007**, *7*, 2499.
[20] S. Beeby, *MEMS Mechanical Sensors*, Artech House, Boston, **2004**.
[21] P. J. French, A. G. R. Evans, *Sens. Actuators* **1988**, *15*, 257.
[22] a) C. Canali, D. Malavasi, B. Morten, M. Prudenziati, A. Taroni, *J. Appl. Phys.* **1980**, *51*, 3282; b) M. Prudenziati, B. Morten, F. Cilloni, G. Ruffi, *Sens. Actuators* **1989**, *19*, 401.
[23] S.-W. Kim, W.-J. Eom, J. Choi, J. J. Kim, *Electron. Lett.* **2014**, *50*, 1575.
[24] a) T. Lee, E. K. Jeon, B.-S. Kim, *J. Mater. Chem. A* **2014**, *2*, 6167; b) T. Lee, S. H. Min, M. Gu, Y. K. Jung, W. Lee, J. U. Lee, D. G. Seong, B.-S. Kim, *Chem. Mater.* **2015**, *27*, 3785.
[25] a) L. E. Greene, M. Law, J. Goldberger, F. Kim, J. C. Johnson, Y. Zhang, R. J. Saykally, P. Yang, *Angew. Chem. Int. Ed.* **2003**, *42*, 3031; b) C. Pacholski, A. Kornowski, H. Weller, *Angew. Chem. Int. Ed.* **2002**, *41*, 1188.